NEOPLASIA
www.neoplasia.com

Volume 10 Number 5 May 2008 pp. 439–449 439

Prostate Cancer Cell–Derived Urokinase-Type Plasminogen Activator Contributes to Intraosseous Tumor Growth and Bone Turnover[1]

Zhong Dong*, Allen D. Saliganan*, Hong Meng*, Sanaa M. Nabha*, Aaron L. Sabbota*, Shijie Sheng†, R. Daniel Bonfil*,†,2 and Michael L. Cher*,†,2

*Department of Urology, Wayne State University School of Medicine, Detroit, MI, USA; †Department of Pathology, Wayne State University School of Medicine and The Barbara Ann Karmanos Cancer Institute, Detroit, MI, USA

Abstract

A variety of proteases have been implicated in prostate cancer (PC) bone metastasis, but the individual contributions of these enzymes remain unclear. Urokinase-type plasminogen activator (uPA), a serine protease, can activate plasminogen and stimulate signaling events on binding its receptor uPAR. In the present study, we investigated the functional role of PC cell–associated uPA in intraosseous tumor growth and bone matrix degradation. Using a severe combined immunodeficient–human mouse model, we found that PC3 cells were the major source of uPA in the experimental bone tumor. Injection of uPA-silenced PC3 cells in bone xenografts resulted in significant reduction of bone tumor burdens and protection of trabecular bones from destruction. The suppressed tumor growth was associated with the level of uPA expression but not with its activity. An increase in the expression of PAI-1, the endogenous uPA inhibitor, was found during *in vitro* tumor-stromal interactions. Up-regulation of PAI-1 in bone stromal cells and preosteoclasts/osteoblasts was due to soluble factor(s) released by PC cells, and the enhanced PAI-1 expression in turn stimulated PC cell migration. Our results indicate that both tumor-derived uPA and tumor-stroma–induced PAI-1 play important roles in intraosseous metastatic PC growth through regulation of a uPA–uPAR–PAI-1 axis by autocrine/paracrine mechanisms.

Neoplasia (2008) 10, 439–449

Introduction

Bone metastasis is the most common complication that significantly contributes to the mortality in prostate cancer (PC) patients, with no curative treatment of the advanced disease. Once disseminated to the bone, the metastatic prostate cancer cells interact with resident cells, and an enhanced expression and activity of proteases that degrade bone matrix and activate growth factors for cancer cell proliferation is frequently observed. This osteolytic response is a prerequisite for the generation of the osteoblastic lesions usually found in PC patients with skeletal metastasis [1,2]. Different proteases such as matrix metalloproteinases and cathepsins have been implicated in PC bone metastasis based on our previous studies [3–6]. Another important protease, urokinase plasminogen activator (uPA) was also reported to be correlated with prostatic malignancy and PC invasion [7,8]. In PC patients, uPA expression was found to be higher in bone metastases than in primary tumors [9]. Moreover, PC patients with skeletal metastasis showed high levels of circulating uPA [10,11].

The uPA system consists of uPA, its receptor (uPAR), plasminogen, and plasminogen activator inhibitors (PAIs). uPA is secreted as a zymogen (pro-uPA), and activation of pro-uPA is accelerated by its

Abbreviations: CM, conditioned medium; GAPDH, glyceraldehyde phosphate dehydrogenase; MVD, microvascular density; PAI, plasminogen activator inhibitor; PC, prostate cancer; RT-PCR, reverse transcription–polymerase chain reaction; SCsi, scrambled siRNA; siRNA, small interfering RNA; uPA, urokinase plasminogen activator; uPAR, urokinase plasminogen activator receptor

Address all correspondence to: R. Daniel Bonfil, PhD, Departments of Urology and Pathology, Wayne State University School of Medicine, 540 E. Canfield Ave., Room 9105, Detroit, MI 48201. E-mail: dbonfil@med.wayne.edu

[1]This research was supported by a grant from the National Institute of Diabetes and Digestive and Kidney Diseases; National Institutes of Health (grant number RO1-CA067687).

[2]These authors jointly supervised this study and should be considered as senior authors.

Received 3 January 2008; Revised 15 February 2008; Accepted 18 February 2008

DOI 10.1593/neo.08106

binding to uPAR [12]. The active uPA catalyzes the conversion of plasminogen to plasmin, which in turn degrades a variety of matrix proteins because of its broad spectrum of substrate specificities. In addition to the proteolytic activity of uPA in the enzymatic cascade, the binding of uPA to uPAR also results in signaling events leading to angiogenesis [13], chemotaxis [14], cell adhesion [15], and cell proliferation [16]. The multifaceted properties of uPA have made itself a versatile regulator of tumor metastasis at different stages and therefore a potential therapeutic target. The activity and turnover of uPA are regulated by another member of the system, PAI-1, which is the primary endogenous inhibitor of uPA. According to its inhibitory function for uPA, PAI-1 was originally predicted to suppress cancer proliferation and metastasis. However, a growing body of evidence has shown that high levels of PAI-1 indicate a poor prognosis for survival in some human cancers [17–19]. Additionally, host-produced PAI-1 was found to be an important tumor-promoting factor in an experimental mouse model [20].

Despite the clinical reports that described the association between uPA expression and skeletal metastases in PC patients, the functional contribution of tumor-derived uPA in bone metastasis has not been addressed. In the present study, we carried out *in vivo* and *in vitro* experiments to investigate the impact of uPA silencing on the growth of human PC cells within human bone xenografts and tumor-associated bone responses. We demonstrated that down-regulation of tumor-derived uPA significantly reduced PC3 bone tumor burden and protected trabecular bone from destruction. Interestingly, we also showed that tumor-stromal interactions induced the expression of PAI-1, which was responsible for an enhanced cancer cell migration. Our data suggest that tumor-derived uPA is one of the dominant factors facilitating metastatic osseous cancer growth.

Materials and Methods

Cell Lines and Stable Transfections

PC3, an androgen-independent cell line derived from a bone metastasis of human prostate adenocarcinoma [21], was purchased from American Type Culture Collection (ATCC, Manassas, VA). It was maintained in RPMI 1640 (Invitrogen Life Technologies, Carlsbad, CA) supplemented with 10% FBS (Atlanta Biologicals, Lawrenceville, GA). An immortalized human bone marrow mesenchymal cell (BMSC) line [22] was kindly given by Dr. Dario Campana (St Jude Children's Research Hospital, Memphis, TN), and maintained in RPMI 1640 supplemented with 10% FBS and 1 nM hydrocortisone (Sigma-Aldrich, St. Louis, MO). BMA3.1A7 (BMA), a macrophage cell line derived from murine bone marrow (preosteoclast) [23], was a generous gift from Dr. Kenneth Rock (Dana-Farber Cancer Institute, Boston, MA). This cell line was maintained in RPMI 1640 supplemented with 10% FBS. MC3T3-E1 subclone 4 (3T3), a murine preosteoblast cell line [24], was purchased from ATCC, and maintained in α-minimum essential medium (Invitrogen Life Technologies) supplemented with 10% FBS. Murine BMA and 3T3 cells were used in our studies because of the current unavailability of human preosteoclast/osteoblast cell lines.

A uPA small interfering RNA (siRNA)–expressing DNA insert was constructed into the p*Silencer* 4.1-CMV plasmid vector (Ambion, Austin, TX), and the selected uPA target sequence was 5′-TGA GAG CCC TGC TGG CGC GCC-3′. The vector containing the uPA siRNA (uPAsi)–expressing insert was amplified, purified, and sequenced. PC3 cells were transfected with either the uPAsi-expressing vector or a vector expressing a scrambled siRNA (SCsi) that did not affect uPA expression. The transfected cells were selected by geneticin treatment, and the resistant cells were further cloned. The cloned cells were seeded into T-75 flasks separately and cultured until about 80% confluence, followed by incubation with serum-free RPMI for 24 hours. Total RNAs and cell lysates were prepared for reverse transcription–polymerase chain reaction (RT-PCR), real-time PCR, and immunoblot analysis.

Mice and Establishment of PC3 Human Bone Tumors

Five-week-old male homozygous C.B-17 *scid/scid* (severe combined immunodeficient [SCID]) mice were purchased from Taconic Farms (Germantown, NY) and allowed to acclimate for 1 week. All procedures involving mice were performed according to the National Institutes of Health standards established in the Guidelines for the Care and Use of Experimental Animals and were approved by the Animal Investigation Committee at Wayne State University School of Medicine.

Intraosseous prostate tumors were generated using the SCID-human model, as described previously [3]. Briefly, SCID mice were subcutaneously implanted with one quarter of human male fetal femur obtained from elective pregnancy terminations (20 to 22 weeks of gestation). The specimens were obtained from Advanced Bioscience Resources (Alameda, CA) in compliance with state and federal regulations. After a 4-week engraftment, the marrow of the bone xenograft was injected with 20 μl of serum-free medium containing 1×10^5 PC cells or no cells (control bone group). We first assessed uPA expression/activity and PAI-1 expression in bone tumors formed by inoculation of parental PC3 cells and in control bones injected only with serum-free medium. Each of the two groups had five mice. Next, we compared the tumor burden and bone degradation in bone tumors generated by the injection of PC3-derived uPAsi clones and SCsi clones (negative control expressing a SCsi), with eight animals in each group.

Preparation of Tissue Extracts and Paraffin Sections

Three weeks after the intraosseous PC3 cell injections, implanted control bone fragments and bone tumors were harvested. Each specimen was longitudinally cut into two pieces. One piece was immediately homogenized with 500 μl of tissue lysis buffer (150 mM NaCl, 20 mM Tris, pH 7.5, 1% NP40, and 5 mM EDTA) in a mortar (CoorsTek, Golden, CO). The homogenate was centrifuged at 10,000 rpm at 4°C for 10 minutes, and the supernatant was collected and stored at −80°C. The other piece of tissue was fixed in 4% paraformaldehyde overnight and decalcified for 2 weeks with 10% EDTA (pH 6.5) in PBS. The decalcified tissue was dehydrated, infiltrated, and paraffin-embedded. Tissue sections (5 μm) were prepared.

Cocultures and Treatment with Conditioned Media

For coculture studies, PC3 parental cells were seeded alone or together with BMSCs, BMA, or 3T3 cells (10^5 cells/well per cell type) in RPMI 1640 medium supplemented with 10% FBS in 24-well plates. Twenty-four hours later, the medium was discarded, and the cells were washed once with PBS. Five hundred microliters of serum-free RPMI 1640 medium were added to each well, and the cells were cultured at 37°C for 48 hours. Conditioned media (CM) were collected, clarified by centrifugation, and subjected to immunoblot analysis for uPA and ELISA for PAI-1.

For experiments involving treatment with CM, PC3 and BMSCs were seeded separately into T-75 flasks and cultured until approximately 80% confluence. The cells were then incubated with serum-free

RPMI for 48 hours. The CM were collected and clarified by centrifugation. PC3 cells and BMSCs were seeded separately into a 24-well plate (10^5/well) for 24 hours and then treated with the CM collected from the other cell type for 48 hours. Total RNA samples were prepared from the cells for RT-PCR.

Semiquantitative RT-PCR and Real-time PCR

Total RNA samples were extracted from the different cells using TRIzol reagent (Invitrogen Life Technologies), according to the manufacturer's instructions. The primers used for both RT-PCR and real-time PCR were as follows: uPA forward 5′-GTC TAC CTG GGT CGC TCA AG-3′ and reverse 5′-CAC AGC ATT TTG GTG GTG AC-3′; uPAR forward 5′-CTG GAG CTG GTG GAG AAA AG-3′ and reverse 5′-TGT TGC AGC ATT TCA GGA AG-3′; PAI-1 forward 5′-GAA CTT CAG GAT GCA GAT G-3′ and reverse 5′-CTG ATC ATA CCT TTT GTG TG-3′; glyceraldehyde phosphate dehydrogenase (GAPDH) forward 5′-AAG GTC ATC CCT GAG CTG AA-3′ and reverse 5′-CTG ATC ATA CCT TTT GTG TG-3′.

For RT-PCR, the Reverse-iT One-Step RT-PCR kit (ABgene, Rochester, NY) was used, and the cycle parameters were as follows: 47°C for 30 minutes for the first strand of cDNA synthesis; 94°C for 15 minutes for reverse transcription inactivation; 94°C for 20 seconds for denaturation; 60°C for 30 seconds for annealing; and 72°C for 1 minute for extension. Amplification was carried out with 19 cycles for uPA (374-bp product) and GAPDH (271-bp product), and 30 cycles for PAI-1 (525-bp product). PCR products were resolved on a 1% agarose gel by electrophoresis, and visualized by ethidium bromide staining.

For real-time PCR, the Mx4000 Multiplex Quantitative PCR System and Brilliant SYBR Green QPCR Master Mix (Stratagene, La Jolla, CA) were used to quantitate uPAR and PAI-1 mRNA expression in PC3 clones. The experiments were performed as described previously [25]. The relative mRNA levels of the target genes were calculated using threshold cycles (C_t) and normalized by internal control gene GAPDH. The formula for the calculation was $2^{[\text{target gene } Ct \text{ (scrambled clone)} - \text{target gene } Ct \text{ (silenced clone)}]}/2^{[\text{GAPDH } Ct \text{ (scrambled clone)} - \text{GAPDH } Ct \text{ (silenced clone)}]}$.

Immunoblot Analysis

Cell or tissue lysates obtained from different experiments were measured for total protein concentrations using the bicinchoninic acid assay (Pierce Chemical Company, Rockford, IL). Equal amount of cell or tissue lysate protein was electrophoresed and transferred to nitrocellulose membranes. The membranes were incubated with primary monoclonal antibodies against either human uPA (1 μg/ml; EMD Chemicals Inc., San Diego, CA), human uPAR (1 μg/ml; American Diagnostica Inc., Stamford, CT), or human cytokeratins (1:3000; Sigma-Aldrich). The membranes were then incubated with a secondary antibody conjugated with horseradish peroxidase (Cell Signaling Technology, Danvers, MA). The specific bands were developed on autoradiography films by treatment of the membranes with enhanced chemiluminescent substrate (Pierce). The membranes were stripped and reprobed with an antibody to β-actin (1:5000; Sigma-Aldrich), used as a loading control. To compare the relative uPA expression among different groups of PC3 bone tumors, the intensities of specific uPA and cytokeratin bands in immunoblots were measured (total pixel count of each band) using UN-SCAN-IT software (Silk Scientific, Orem, UT). Data were presented as a ratio of uPA band intensities to cytokeratin band intensities.

uPA Activity Assay

uPA activity in the cell or tissue lysates was measured using the Urokinase Activity Assay kit (EMD Chemicals Inc.), following the manufacturer's instructions. The assay measures only the active species of uPA, and a standard curve was generated using recombinant active uPA. The assay condition was optimized so that the amount of the tissue extract or cell extract added gave rise to a uPA activity within the linear range of the detection. Each reaction was performed in duplicate.

PAI-1 ELISA

Human IMUBIND Tissue PAI-1 ELISA kit (American Diagnostica Inc.) and Mouse PAI-1 Total Antigen ELISA Kit (Innovative Research Inc., Southfield, MI) were used to measure PAI-1 expression in CM and cell or tissue lysates, following the manufacturer's instructions. Both kits have been shown to detect the latent and active forms of PAI-1 and uPA-bound PAI-1 in tissue extracts and cell culture supernatants and do not cross-react with PAI-2. A standard curve was generated using recombinant PAI-1. The assay conditions with both kits were optimized to ensure PAI-1 detection in the linear range. All reactions were performed in duplicates.

Immunohistochemistry

Paraffin sections prepared from control bones and PC3 bone tumors were deparaffinized and rehydrated and were then incubated with monoclonal antibodies against either human uPA (20 μg/ml; American Diagnostica Inc.) or human PAI-1 (40 μg/ml; American Diagnostica Inc.). After incubations with the secondary antibody, the immunoreactivity was developed by addition of 3,3-diaminobenzidine, and sections were counterstained with Mayer's hematoxylin. Negative controls were slides incubated with preimmune mouse immunoglobulin (e-Bioscience, San Diego, CA) in place of primary antibodies. Intratumoral microvascular density (MVD) was assessed using immunohistochemistry as described previously [26]. Briefly, sections were incubated with a monoclonal antibody against human CD34 (clone QBEND 10; 1:50 dilution; DAKO, Carpinteria, CA) after microwave antigen retrieval using Ag Citrus Plus Retrieval Solution (BioGenes, San Ramon, CA). Binding of the antibody to CD34 was demonstrated using EnVision+ System (DAKO) and diaminobenzidine. Three areas with the most prominent CD34-positive endothelial cell clusters (*hot spots*) were identified within the tumor tissue at a low magnification, and the microvessels counted in those areas were identified at a magnification of ×200.

Hematoxylin and Eosin Staining and Histomorphometry

Paraffin sections were stained with hematoxylin and eosin (H&E). Digital photomicrographs were captured under a magnification of ×5 using a microscope (Zeiss Axioplan 2; Zeiss, Gottingen, Germany) equipped with a software-controlled digital camera (Axiovision; Zeiss). All ×5-microscopic fields in each longitudinal section were analyzed. The percentage occupied by tumor and trabecular bones in the entire section of the slide was calculated by the software.

Cell Proliferation Assay

PC3-derived SCsi and uPAsi clones were plated separately into 24-well plates (2×10^4/ml per well) in RPMI 1640 supplemented with geneticin.

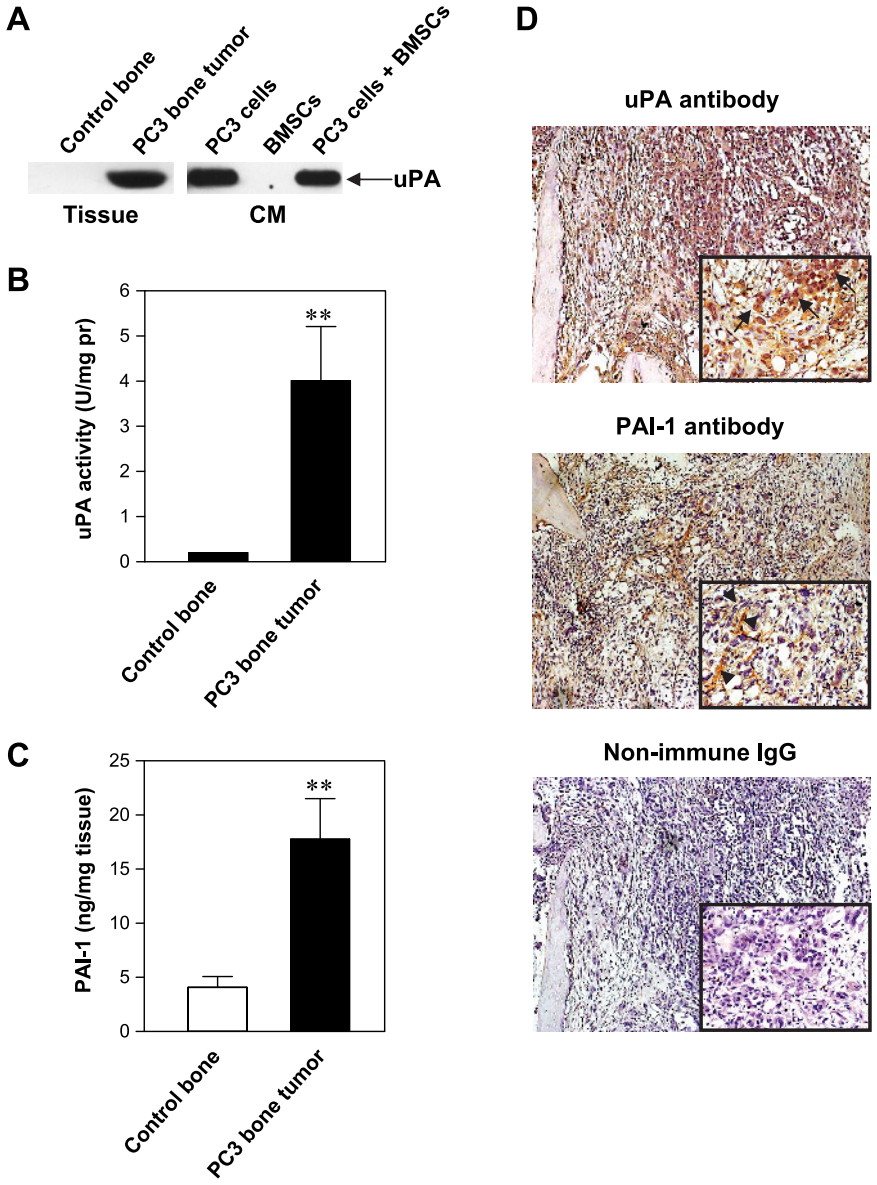

Figure 1. uPA protein expression in representative tissue samples and CM (A); uPA activity in the tissue samples (B); PAI-1 protein quantification in the tissue samples (C), $**P < .01$; and immunohistochemistry of representative samples of PC3 bone tumors (D). Arrows indicate PC3 tumor cells; arrowheads, stromal cells and bone matrix fibers. Original magnifications, ×100 and ×400.

On days 2, 4, and 6, three wells for each clone were counted using a hematocytometer, and the mean number of the cells was calculated.

RNA Interference and Cell Motility Assay

A validated human PAI-1 siRNA (sense 5′-GCC AGA UUC AUC AUC AAU Gtt-3′ and antisense 5′-CAU UGA UGA UGA AUC UGG Ctc-3′) and a control siRNA were purchased from Ambion. Bone marrow mesenchymal cells (10^5/well) were seeded into a 24-well plate and cultured overnight. The next day, the cells were washed once with PBS and treated with 80 nM of either PAI-1 siRNA or control siRNA for 24 hours. To perform the cell motility assay, siRNA-treated BMSCs growing in 24-well plates were washed once with PBS and 500 μl of serum-free RPMI 1640 medium were added to each well. Cell culture inserts with 8-μm pores (BD Falcon, Treyburn, NC) containing 10^5 PC3 cells in 1 ml of serum-free RPMI 1640 were placed in these wells. Controls for spontaneous transmigration included inserts with PC3 cells but no BMSCs in the bottom well. After incubation at 37°C for 16 hours, the upper face of the insert membrane was wiped off using a cotton swab to remove the cells, and the lower face of the membrane was stained with Diff-Quik kit (Dade Behring Inc., Newark, DE). The migrated cells in the center of the membrane were counted under a microscope at a magnification of ×400 in 10 consecutive fields, each of which equaled to 0.06 mm^2. The mean number of traversing cells was calculated.

Statistical Analysis

Data comparing differences between two groups were statistically analyzed using unpaired Student's *t*-test. Multiple comparisons were made using one-way analysis of variance. Differences were considered significant when $P < .05$.

Results

uPA Expression, Activity, and PAI-1 Induction in PC3 Human Bone Tumors

Tissue lysates obtained from intraosseous tumors generated by parental PC3 cell inoculation and from control bone xenografts were assessed for uPA expression and activity. As shown in Figure 1*A*, uPA protein was only detected in the tissue lysate prepared from PC3 bone tumors. These results are in agreement with the data obtained from our *in vitro* studies with PC3 cells and BMSCs cultured alone or together (Figure 1*A*). uPA activity assay revealed corresponding uPA enzymatic activity in the PC3 bone tumors but minimum activity in the control bones (Figure 1*B*). In addition, PAI-1 expression was significantly induced in the PC3 bone tumor when compared with the control bone ($P < .01$) (Figure 1*C*). Immunohistochemical analysis of PC3 bone tumor tissues showed that uPA was predominantly expressed by PC3 tumor cells, whereas PAI-1 was mainly localized to stromal cells and matrix fibers and shown to be weaker in PC3 tumor cells (Figure 1*D*).

Characterization of PC3 Cells Expressing uPA Silencing RNA

Because tumor cells were the major source of uPA in the PC3 bone tumors, we applied the RNA interference technique to specifically down-regulate uPA in PC3 cells. Clones obtained by transfection of PC3 cells with either the vector expressing uPA siRNA or the vector expressing SCsi were selected, and total RNA and protein samples were prepared. RT-PCR analysis revealed a group of PC3 clones with reduced levels of uPA mRNA expression due to uPA silencing (uPAsi C2, C3, and C6) compared with the clone expressing SCsi (SCsi C3; Figure 2*A*). Immunoblot analysis further

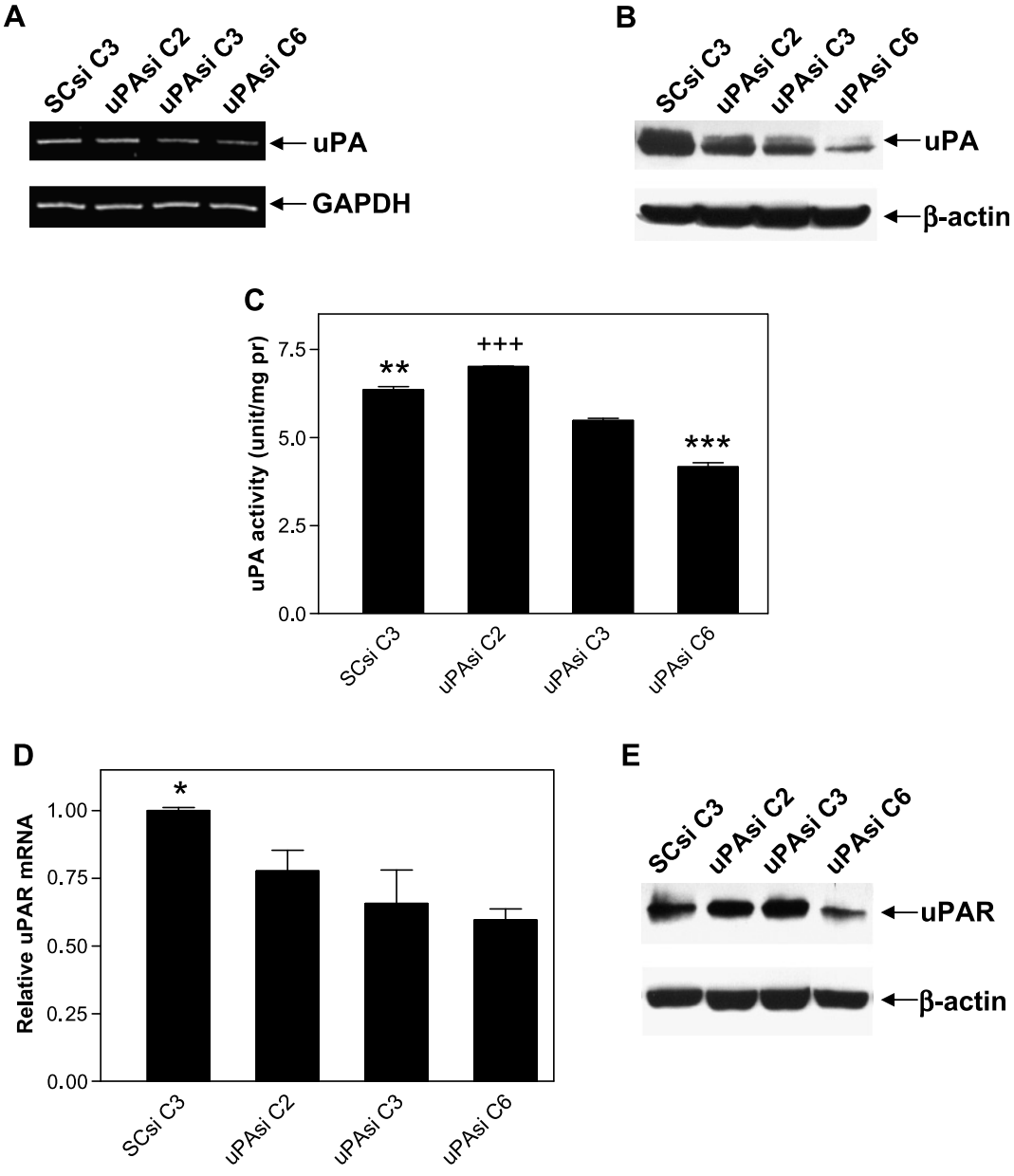

Figure 2. Expression of uPA mRNA (A), protein (B), and enzymatic activity (C), ***$P < .001$ when compared with other three groups; **$P < .01$ when compared with uPAsi C2 or C3; $^{+++}P < .001$ when compared with uPAsi C3; expression of uPAR mRNA (D) and protein (E) in PC3 clones, *$P < .05$ when compared with uPAsi C3 or C6.

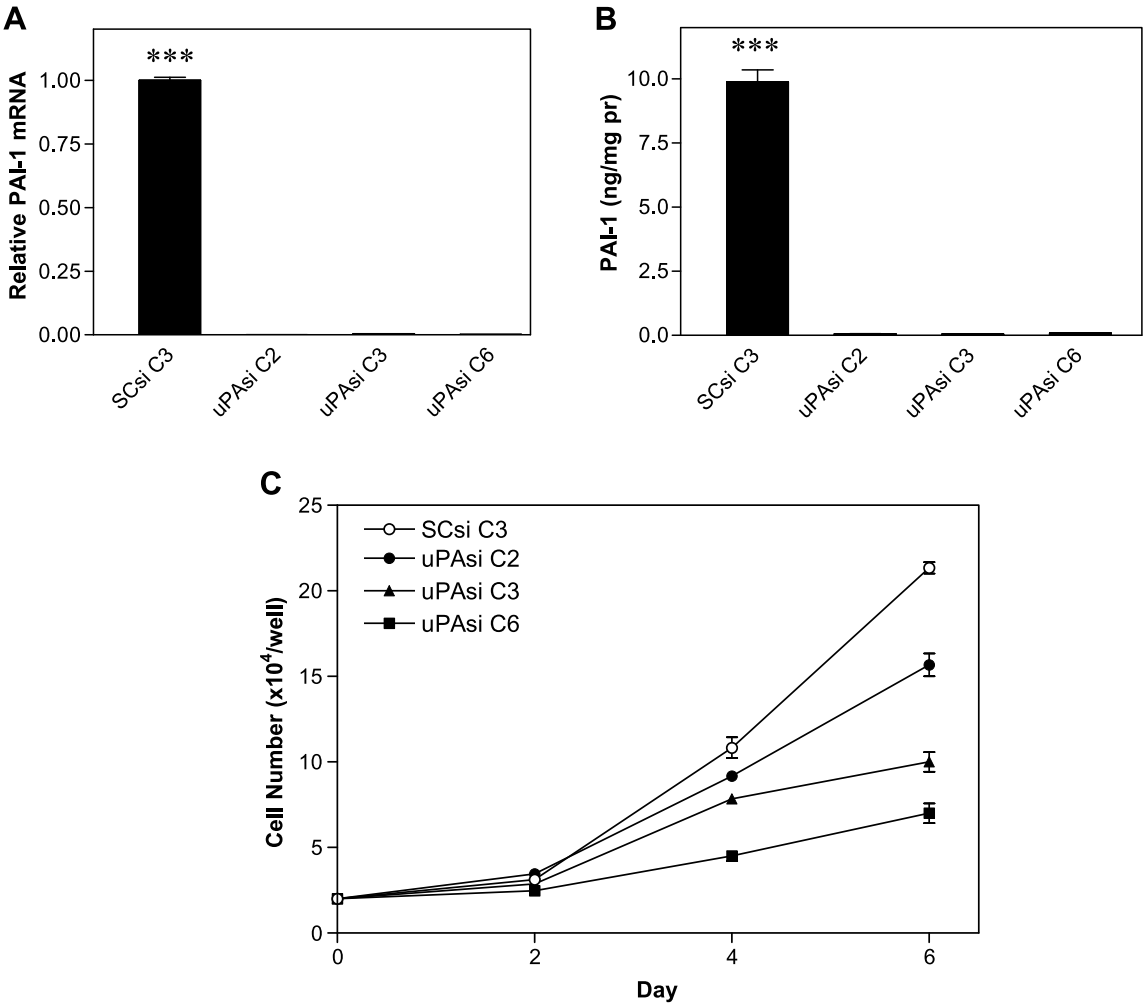

Figure 3. mRNA expression (A) and protein quantification (B) of PAI-1 in PC3 clones, ***$P < .001$ when compared with other three groups; and proliferation rates of PC3 clones (C).

confirmed the inhibition of uPA expression in uPAsi clones at the protein level, with decreasing intensity of the specific band from C2 to C6 (Figure 2*B*). The specific activity assay showed a gradual reduction of uPA activity in these clones consistent with their respective uPA expression ($P < .001$; Figure 3*C*), although uPA activity in the uPAsi clone 2 was slightly higher than that in the SCsi control clone (Figure 2*C*). Real-time PCR and immunoblot analyses of uPAsi clones revealed a similar trend for uPAR (Figure 2, *D* and *E*). We also checked PAI-1 expression at both mRNA and protein levels in the clones. As shown in Figure 3*A*, there was significant reduction of PAI-1 mRNA expression in uPAsi clones when compared with that in the SCsi clone ($P < .001$). Results from ELISA displayed an identical pattern of PAI-1 expression at the protein level (Figure 3*B*).

To evaluate the growth effect of uPA silencing on the PC3 clones, we performed a cell proliferation assay. As shown in Figure 3*C*, the proliferation rate of uPAsi PC3 cells was retarded by uPA downregulation and correlated with the level of uPA expression.

Inhibition of PC3 Bone Tumor Proliferation and Trabecular Bone Degradation By uPA Silencing

To investigate the role of tumor-derived uPA in PC bone tumor growth and subsequent bone turnover, we carried out an *in vivo* experiment using the uPA silenced PC3 clones. Human fetal bone fragments were implanted into SCID mice, and the uPAsi or SCsi PC3 cells were injected into the implanted human fetal bone xenografts 4 weeks later. Three weeks after PC3 cell inoculation, the fetal bone fragments were harvested and processed for histologic and biochemical studies. The bone xenografts injected with the SCsi PC3 clone exhibited aggressive bone tumor growth and trabecular bone degradation by H&E staining. On the contrary, the bones injected with PC3 clones silenced for uPA showed smaller tumors and reduced matrix degradation (Figure 4*A*). Immunoblot analysis of tissue lysates from individual bone xenografts using the uPA monoclonal antibody revealed lower uPA expression in the uPAsi clones than that in the SCsi clone (Figure 4*B*). The epithelial marker cytokeratin was also detected in these samples and used as an indicator of PC3 tumor cells. The intensities of specific cytokeratin bands in the SCsi bone tumor group were relatively higher than that in the uPAsi groups. To compare the relative uPA expression in the bone tumors among different groups, the specific bands from both uPA and cytokeratin were scanned, and the ratios of uPA to cytokeratin intensities were calculated. As shown in Figure 4*B*, the uPA expression was dramatically reduced in uPAsi C3 and C6 bone tumors when compared to that in SCsi bone tumors. We further performed histomorphometrical analysis to quantify the bone tumor burden and the area occupied by trabeculae. As shown in Figure 5*A*, uPA silencing significantly reduced

the size of PC3 bone tumors when compared with that generated by the SCsi clone ($P < .01$ between uPAsi C2 and SCsi; and $P < .001$ between uPAsi C3 or C6 and SCsi). This inhibitory effect on tumor growth was associated with reduced levels of uPA expression, as the clones expressing lower levels of uPA generated smaller tumors. Subsequently, the degradation of trabecular bones in the uPAsi PC3 bone tumors was less severe than that in the SCsi PC3 bone tumors ($P < .05$, between uPAsi C3 or C6 and SCsi; Figure 5*B*). These data suggest that the protective effect on trabecular bones was likely to result directly from uPA silencing. To investigate the effect of uPA silencing on intraosseous tumor angiogenesis, we assessed the MVD in the bone tumors from each group. The results obtained showed no significant differences in MVD among the groups (data not shown).

Up-regulation of PAI-1 By In Vitro *PC Cell–Bone Cell Interactions*

As shown earlier in Figure 1*C*, PAI-1 expression was significantly higher in PC3 bone tumors than in control bone xenografts. To

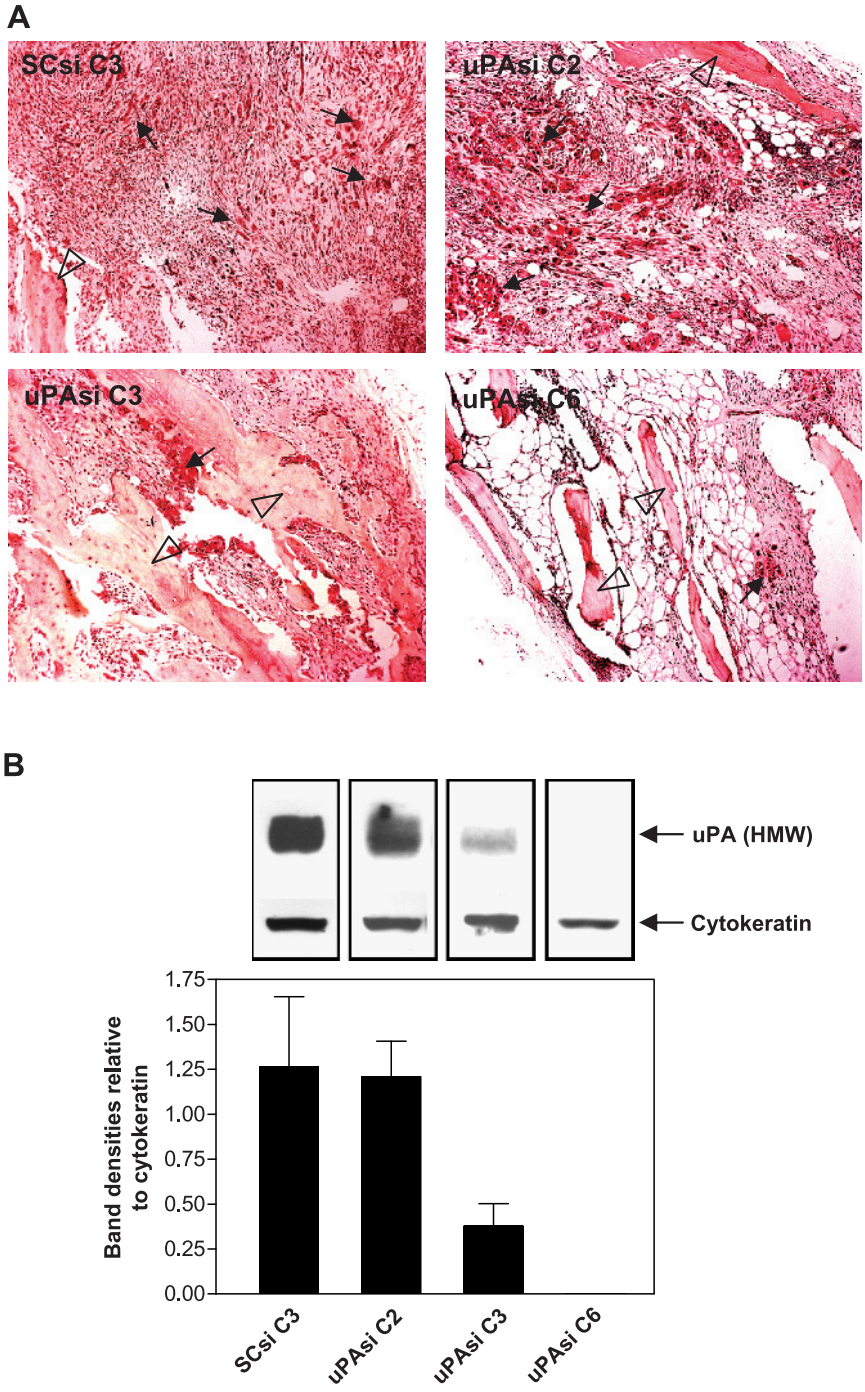

Figure 4. (A) H&E staining of PC3 bone tumor tissues obtained from human fetal bone xenografts injected with PC3 clones (representative samples). Original magnification, ×100. Arrows and clear arrowheads point tumor cells and bone trabeculae, respectively. (B) Relative expression of uPA and cytokeratin in tissue lysates prepared from the PC clone bone tumors. Data are presented as mean ± SE ratio of uPA band intensities to cytokeratin band intensities.

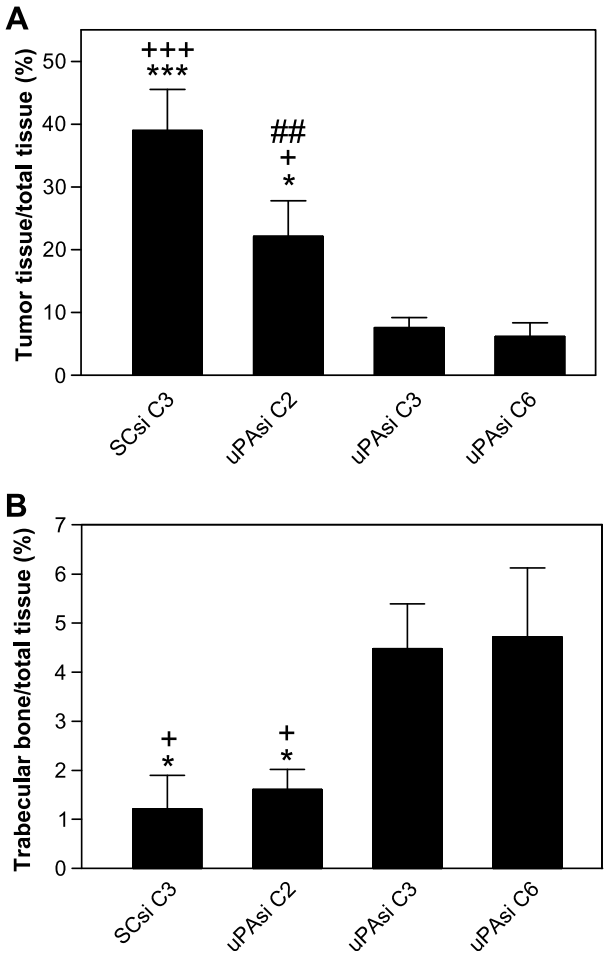

Figure 5. Tumor burden (A) and trabecular degradation (B) in PC3 bone tumors obtained from human fetal bone xenografts injected with PC3 clones, $^{*}P < .05$ and $^{***}P < .001$, when compared with uPAsi C6; $^{+}P < .05$ and $^{+++}P < .001$, when compared with uPAsi C3; $^{\#\#}P < .01$ when compared with SCsi C3.

explore whether this result could be due to PAI-1 induction, we conducted *in vitro* coculture experiments of PC3 and BMSCs. As shown in Figure 6*A*, the interaction of PC3 cell with bone stromal cells led to a dramatic increase in PAI-1 expression ($P < .001$). Similarly, cocultures of PC3 cells with either mouse 3T3 preosteoblasts or mouse BMA preosteoclasts also enhanced mouse PAI-1 expression ($P < .001$ and $P < .05$, respectively; Figure 6*B*). We then collected PC3 or BMSC CM and applied the CM from one cell type to the culture of the other cell type. The results showed that only the CM from PC3 cells stimulated PAI-1 mRNA expression in BMSC, whereas the CM from BMSC did not change PAI-1 mRNA expression in PC3 cells (Figure 6*C*).

Stimulation of PC3 Cell Migration By PAI-1 from BMSCs

Next, we tested the effect of induced PAI-1 from BMSC on PC3 cell motility. BMSCs were treated with the specific human PAI-1 siRNA for 24 hours, which confirmed down-regulation of PAI-1 mRNA (Figure 7*A*). *In vitro* assays were used to quantitate PC3 cell motility across the filter with 8-μm pores toward BMSCs. We found that BMSCs stimulated the migration of PC3 cells when compared to the spontaneous PC3 cell migration (with no BMSC in the bottom well), and the induction of PC3 cell motility was almost completely abolished when BMSCs were pretreated with the specific PAI-1 siRNA ($P < .01$; Figure 7*B*).

Discussion

Overexpression of uPA has been reported in primary PC and bone metastasis [7–9,27]. Because the precise pathologic role of tumor-derived uPA in PC bone metastasis is still unclear, here we investigated the effect of silencing PC3 uPA expression on intraosseous tumor growth. This cell line was of choice for our study, because it was initiated from a bone metastasis of a PC patient and it has the highest uPA expression among the three most used PC cell lines, namely, LNCaP, DU145, and PC3 [28,29]. Our *in vivo* data with parental PC3 cells indicate that cancer cells are the major source for uPA when they proliferate in the implanted bone. These results were confirmed by our coculture studies using PC3 and BMSCs.

Characterization of PC3-derived transfected clones revealed an association between uPA silencing and the reduction of uPA mRNA and protein expression. Interestingly, uPA C2 showed even higher uPA activity than the control PC3 clone (SCsi C3). This finding could be potentially ascribed to different PAI-1 levels in those two clones, as PAI-1 can bind active uPA and inhibit its activity [30]. Indeed, significant down-regulation of PAI-1 expression was revealed by ELISA in all three uPAsi clones. Although uPAsi C2 had relatively lower uPA expression than SCsi C3 due to siRNA silencing, its PAI-1 expression was much lower than that from SCsi C3, which led to more free uPA molecules unbound by PAI-1 and therefore higher uPA activity in uPAsi C2. The other two uPAsi clones also exhibited similar reduction of PAI-1 to uPAsi C2, but their uPA expression was substantially silenced. Therefore, the reduction of net uPA activity in uPAsi C3 and C6 was mainly due to the reduced uPA synthesis. Furthermore, low concentrations of uPA in uPAsi C3 and C6 might promote binding of PAI-1, although also at very low concentrations, to uPA/uPAR and trigger the formation of trimeric complex uPA/uPAR/PAI-1, leading to internalization and degradation of both uPA and PAI-1 [31].

Our *in vivo* silencing experiment used several uPAsi PC3 clones with different levels of uPA down-regulation to investigate the precise role of uPA in intraosseous PC3 tumor growth and bone matrix degradation. Quantifications of tumor and trabecular bone areas by histomorphometric analysis showed significant reduction of bone tumor burdens and remarkable protection of trabecular bones by uPA silencing. The use of siRNA to target uPA expression has been reported in other experimental tumor models. For instance, intraperitoneal injection of a vector expressing uPA and uPAR siRNA reduced preestablished intracranial growth of gliomas in nude mice [32], and intratumoral injection of a plasmid construct expressing uPA and uPAR siRNA completely inhibited established orthotopic PC3 tumors in immunosuppressed mice [33]. Our study differs from those mentioned previously in that we specifically silenced uPA in prostate cancer cells that represent the major source of this serine protease in intraosseous tumors. Knockdown of tumor-associated uPA was sufficient to achieve a significant reduction of intraosseous PC growth and bone degradation in the SCID-human model of PC skeletal metastasis. To our knowledge, this is the first study that revealed a functional role for PC cell–derived uPA in intraosseous tumor growth and bone turnover.

The establishment and growth of metastatic cancer cells in the bone marrow require osteolysis for their physical expansion, and

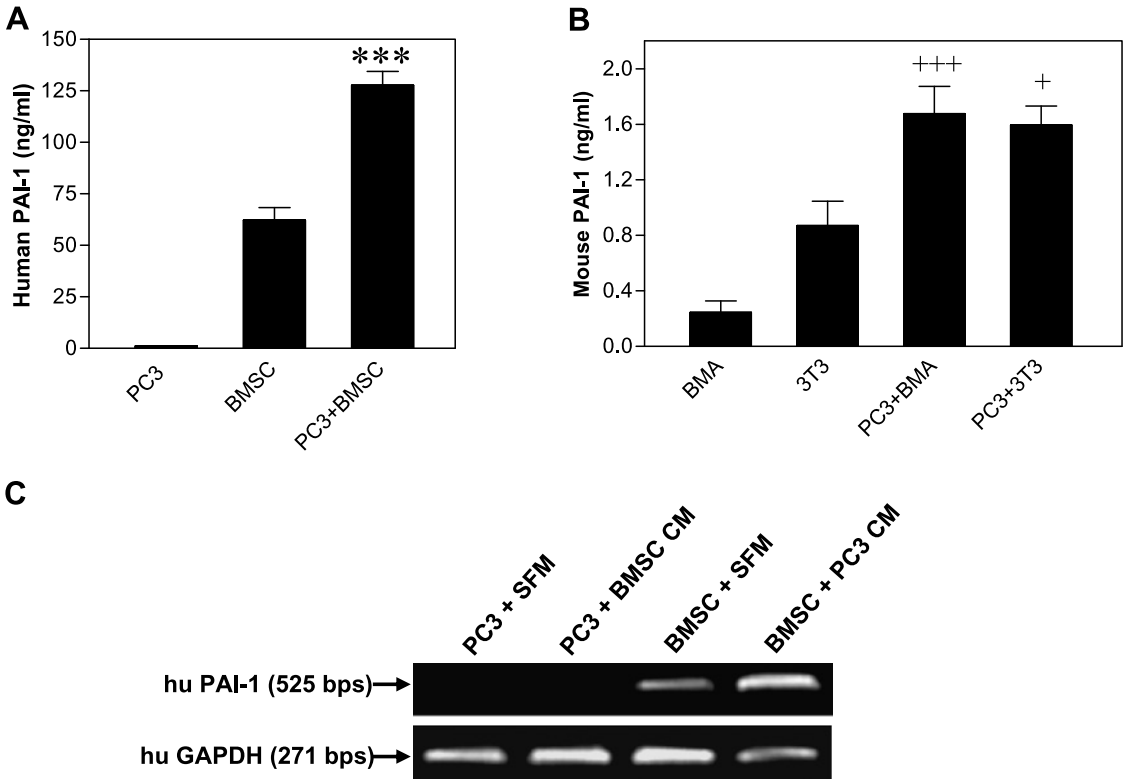

Figure 6. PAI-1 expression in the cocultures of PC3 cells with human BMSCs (A) or with mouse osteoclasts/osteoblasts (B), $^{***}P < .001$ when compared with the remaining groups, $^{+++}P < .001$ when compared with BMA, $^{+}P < .05$ when compared with 3T3; and PAI-1 mRNA expression in BMSCs treated with PC3 CM (C).

the calcium and marrow-derived growth factors released by matrix degradation provide living supports for the metastatic cancer cell proliferation [34]. The serine protease uPA specifically activates plasminogen into active plasmin, which in turn cleaves a variety of extracellular matrix substrates such as fibronectin, vitronectin, and fibrin [35]. In addition, uPA is also involved in many biologic functions, as it regulates growth factor activation, cell adhesion, chemotaxis, and angiogenesis [36,37]. In the current study, we found that the *in vitro* proliferation rate of PC3 clones was closely associated with uPA expression but not with uPA activity. This is further confirmed by our *in vivo* experiment that showed an association between uPA expression and intraosseous tumor burdens, whereas uPA activity revealed no significant changes among different groups (data not shown). Achbarou et al. [38] found that the enzymatic activity

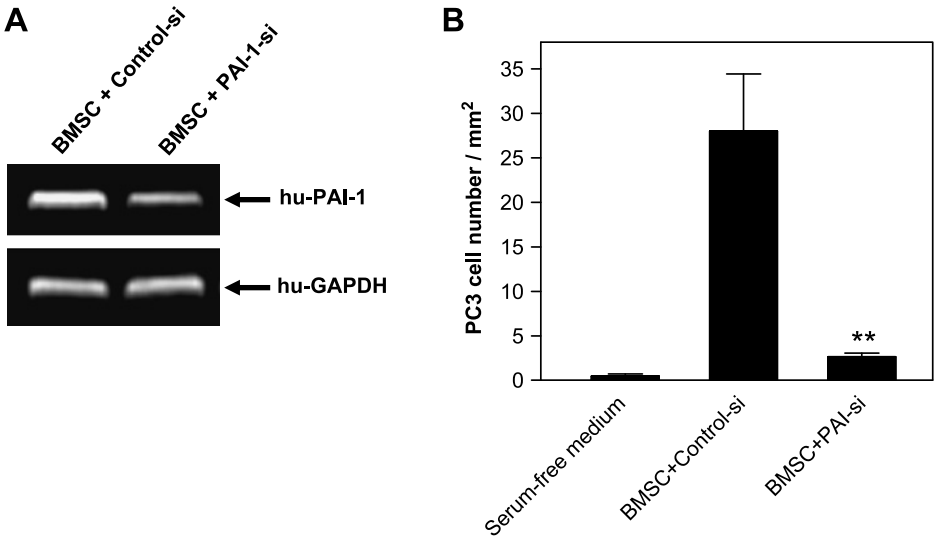

Figure 7. Expression of PAI-1 mRNA in BMSCs treated with PAI-1 siRNA (A) and PC3 cell motility assay (B), $P < .01$ when compared with control siRNA-treated PC3 cells.

of uPA promotes PC cell intravasation into the vasculature and extravasation into bone tissue. However, our *in vivo* model is used to study the last stage of skeletal metastasis, namely intraosseous tumor growth, in which degradation of basement membrane might not be necessary. At this stage, the expression of uPA, rather than its activity, may be more important for maintaining continuous tumor proliferation. The growth-stimulating effect of uPA on tumor cells has been previously reported, and it was found that either application of uPA siRNA or stable transfection of a vector expressing uPA siRNA remarkably reduced cell growth rates of a breast cancer cell line [39] and a hepatocellular carcinoma cell line [40]. This effect was initiated by binding of the uPA growth factor domain to its receptor uPAR, and there was no uPA activity needed for this process [29,41,42]. Interestingly, it was found that uPAR expression was also regulated by uPA. Mahanivong et al. [43] demonstrated that the introduction of uPA antisense RNA to human breast cancer cells reduced not only uPA but also uPAR expression in these cells and that this inhibition could be reversed by the addition of soluble single-chain uPA to the cell culture system. Our data collected from real-time PCR showed a concomitant down-regulation of uPAR mRNA by uPA silencing, which was confirmed at the protein level (uPAsi C6) by immunoblot. These findings further suggest that uPA silencing attenuates the number of uPA-uPAR complex and therefore reduces signaling stimulation for cell growth.

uPA is regulated at different levels for its expression and activity. After activation, uPA activity can be inhibited by its endogenous inhibitors. PAI-1, albeit a predominant uPA inhibitor, has been reported to be overexpressed in a variety of neoplasms such as breast [44], lung [45], colon [46], ovary [47], kidney [48], and oral [49] cancers. Usher et al. [50] detected PAI-1 mRNA and protein expression in specimens obtained from 13 of 16 prostate cancer patients and found the localization in fibroblast like cells. Our studies revealed enhanced PAI-1 expression in intraosseous PC3 tumors, which was verified by our coculture experiments. This up-regulation of PAI-1 was due to soluble factors from PC3 cells that stimulated PAI-1 gene transcription in bone cells. Furthermore, PAI-1 expression was also regulated by uPA because uPA silencing in PC3 cells led to reduction of PAI-1 expression at both the gene and protein levels. These data suggest that PAI-1 expression is regulated by paracrine and autocrine mechanisms. We also investigated the role of PAI-1 in regulation of PC cell motility. We found that soluble factors derived from BMSCs were chemotactic for PC3 cells. Silencing PAI-1 gene in the BMSCs by specific PAI-1 siRNA led to a significant reduction in PC3 cell motility, indicating that PAI-1 was one of the soluble factors that induced PC3 cell migration. A possible mechanism underlying this response could be ascribed to PAI-1's impact on cell attachment [51].

In conclusion, we demonstrated that silencing uPA in PC3 cells led to not only reduced uPA but also suppressed uPAR. These uPA-silenced PC3 cells produced lower tumor burdens and less trabecular bone degradation than the SCsi PC3 control cells. These effects were mainly due to reduced uPA expression rather than inhibited uPA activity. The concomitant uPAR down-regulation by uPA silencing, together with the attenuated PAI-1 induction in bone resident cells, may also contribute to the reduced intraosseous tumor burden. Taken together, these results suggest that both tumor-derived uPA and tumor-stroma–induced PAI-1 play important roles in intraosseous metastatic PC growth through regulation of a uPA–uPAR–PAI-1 axis by autocrine/paracrine mechanisms. Therefore, targeting uPA may provide an effective treatment of the patients with prostate cancer bone metastasis. Our findings in concert with our previous studies on matrix metalloproteinase [3,4] also suggest that although certain protease activities can be crucial for tumor-induced osteolytic responses, expression levels of other proteases such as uPA may have substantial impact on metastatic tumor growth.

References

[1] Percival RC, Urwin GH, Harris S, Yates AJ, Williams JL, Beneton M, and Kanis JA (1987). Biochemical and histological evidence that carcinoma of the prostate is associated with increased bone resorption. *Eur J Surg Oncol* **13**, 41–49.

[2] Keller ET and Brown J (2004). Prostate cancer bone metastases promote both osteolytic and osteoblastic activity. *J Cell Biochem* **91**, 718–729.

[3] Dong Z, Bonfil RD, Chinni S, Deng X, Trindade Filho JC, Bernardo M, Vaishampayan U, Che M, Sloane BF, Sheng S, et al. (2005). Matrix metalloproteinase activity and osteoclasts in experimental prostate cancer bone metastasis tissue. *Am J Pathol* **166**, 1173–1186.

[4] Bonfil RD, Dong Z, Trindade Filho JC, Sabbota A, Osenkowski P, Nabha S, Yamamoto H, Chinni SR, Zhao H, Mobashery S, et al. (2007). Prostate cancer–associated membrane type 1–matrix metalloproteinase: a pivotal role in bone response and intraosseous tumor growth. *Am J Pathol* **170**, 2100–2111.

[5] Podgorski I, Linebaugh BE, Sameni M, Jedeszko C, Bhagat S, Cher ML, and Sloane BF (2005). Bone microenvironment modulates expression and activity of cathepsin B in prostate cancer. *Neoplasia* **7**, 207–223.

[6] Li Y, Che M, Bhagat S, Ellis KL, Kucuk O, Doerge DR, Abrams J, Cher ML, and Sarkar FH (2004). Regulation of gene expression and inhibition of experimental prostate cancer bone metastasis by dietary genistein. *Neoplasia* **6**, 354–363.

[7] Camiolo SM, Markus G, Englander LS, Siuta MR, Hobika GH, and Kohga S (1984). Plasminogen activator content and secretion in explants of neoplastic and benign human prostate tissues. *Cancer Res* **44**, 311–318.

[8] Van Veldhuizen PJ, Sadasivan R, Cherian R, and Wyatt A (1996). Urokinase-type plasminogen activator expression in human prostate carcinomas. *Am J Med Sci* **312**, 8–11.

[9] Kirchheimer JC, Pfluger H, Ritschl P, Hienert G, and Binder BR (1985). Plasminogen activator activity in bone metastases of prostatic carcinomas as compared to primary tumors. *Invasion Metastasis* **5**, 344–355.

[10] Hienert G, Kirchheimer JC, Christ G, Pfluger H, and Binder BR (1988). Plasma urokinase-type plasminogen activator correlates to bone scintigraphy in prostatic carcinoma. *Eur Urol* **15**, 256–258.

[11] Shariat SF, Roehrborn CG, McConnell JD, Park S, Alam N, Wheeler TM, and Slawin KM (2007). Association of the circulating levels of the urokinase system of plasminogen activation with the presence of prostate cancer and invasion, progression, and metastasis. *J Clin Oncol* **25**, 349–355.

[12] Andreasen PA, Egelund R, and Petersen HH (2000). The plasminogen activation system in tumor growth, invasion, and metastasis. *Cell Mol Life Sci* **57**, 25–40.

[13] Basire A, Sabatier F, Ravet S, Lamy E, Mialhe A, Zabouo G, Paul P, Gurewich V, Sampol J, and Dignat-George F (2006). High urokinase expression contributes to the angiogenic properties of endothelial cells derived from circulating progenitors. *Thromb Haemost* **95**, 678–688.

[14] Okada SS, Grobmyer SR, and Barnathan ES (1996). Contrasting effects of plasminogen activators, urokinase receptor, and LDL receptor–related protein on smooth muscle cell migration and invasion. *Arterioscler Thromb Vasc Biol* **16**, 1269–1276.

[15] Chang AW, Kuo A, Barnathan ES, and Okada SS (1998). Urokinase receptor–dependent upregulation of smooth muscle cell adhesion to vitronectin by urokinase. *Arterioscler Thromb Vasc Biol* **18**, 1855–1860.

[16] Kirchheimer JC, Wojta J, Christ G, and Binder BR (1989). Functional inhibition of endogenously produced urokinase decreases cell proliferation in a human melanoma cell line. *Proc Natl Acad Sci USA* **86**, 5424–5428.

[17] Duffy MJ (2002). Urokinase plasminogen activator and its inhibitor, PAI-1, as prognostic markers in breast cancer: from pilot to level 1 evidence studies. *Clin Chem* **48**, 1194–1197.

[18] Kobayashi H, Fujishiro S, and Terao T (1994). Impact of urokinase-type plasminogen activator and its inhibitor type 1 on prognosis in cervical cancer of the uterus. *Cancer Res* **54**, 6539–6548.

[19] Werle B, Kotzsch M, Lah TT, Kos J, Gabrijelcic-Geiger D, Spiess E, Schirren J, Ebert W, Fiehn W, Luther T, et al. (2004). Cathepsin B, plasminogenactivator-inhibitor (PAI-1) and plasminogenactivator-receptor (uPAR) are prognostic factors for patients with non–small cell lung cancer. *Anticancer Res* **24**, 4147–4161.

[20] Maillard C, Jost M, Romer MU, Brunner N, Houard X, Lejeune A, Munaut C, Bajou K, Melen L, Dano K, et al. (2005). Host plasminogen activator inhibitor-1 promotes human skin carcinoma progression in a stage-dependent manner. *Neoplasia* **7**, 57–66.

[21] Kaighn ME, Narayan KS, Ohnuki Y, Lechner JF, and Jones LW (1979). Establishment and characterization of a human prostatic carcinoma cell line (PC-3). *Invest Urol* **17**, 16–23.

[22] Mihara K, Imai C, Coustan-Smith E, Dome JS, Dominici M, Vanin E, and Campana D (2003). Development and functional characterization of human bone marrow mesenchymal cells immortalized by enforced expression of telomerase. *Br J Haematol* **120**, 846–849.

[23] Kovacsovics-Bankowski M and Rock KL (1995). A phagosome-to-cytosol pathway for exogenous antigens presented on MHC class I molecules. *Science* **267**, 243–246.

[24] Wang D, Christensen K, Chawla K, Xiao G, Krebsbach PH, and Franceschi RT (1999). Isolation and characterization of MC3T3-E1 preosteoblast subclones with distinct *in vitro* and *in vivo* differentiation/mineralization potential. *J Bone Miner Res* **14**, 893–903.

[25] Chinni SR, Sivalogan S, Dong Z, Filho JC, Deng X, Bonfil RD, and Cher ML (2006). CXCL12/CXCR4 signaling activates Akt-1 and MMP-9 expression in prostate cancer cells: the role of bone microenvironment–associated CXCL12. *Prostate* **66**, 32–48.

[26] Bonfil RD, Sabbota A, Nabha S, Bernardo MM, Dong Z, Meng H, Yamamoto H, Chinni SR, Lim IT, Chang M, et al. (2006). Inhibition of human prostate cancer growth, osteolysis and angiogenesis in a bone metastasis model by a novel mechanism-based selective gelatinase inhibitor. *Int J Cancer* **118**, 2721–2726.

[27] Cozzi PJ, Wang J, Delprado W, Madigan MC, Fairy S, Russell PJ, and Li Y (2006). Evaluation of urokinase plasminogen activator and its receptor in different grades of human prostate cancer. *Hum Pathol* **37**, 1442–1451.

[28] Helenius MA, Saramaki OR, Linja MJ, Tammela TL, and Visakorpi T (2001). Amplification of urokinase gene in prostate cancer. *Cancer Res* **61**, 5340–5344.

[29] Festuccia C, Dolo V, Guerra F, Violini S, Muzi P, Pavan A, and Bologna M (1998). Plasminogen activator system modulates invasive capacity and proliferation in prostatic tumor cells. *Clin Exp Metastasis* **16**, 513–528.

[30] Ellis V, Wun TC, Behrendt N, Ronne E, and Dano K (1990). Inhibition of receptor-bound urokinase by plasminogen-activator inhibitors. *J Biol Chem* **265**, 9904–9908.

[31] Cubellis MV, Wun TC, and Blasi F (1990). Receptor-mediated internalization and degradation of urokinase is caused by its specific inhibitor PAI-1. *EMBO J* **9**, 1079–1085.

[32] Gondi CS, Lakka SS, Dinh DH, Olivero WC, Gujrati M, and Rao JS (2007). Intraperitoneal injection of a hairpin RNA–expressing plasmid targeting urokinase-type plasminogen activator (uPA) receptor and uPA retards angiogenesis and inhibits intracranial tumor growth in nude mice. *Clin Cancer Res* **13**, 4051–4060.

[33] Pulukuri SM, Gondi CS, Lakka SS, Jutla A, Estes N, Gujrati M, and Rao JS (2005). RNA interference-directed knockdown of urokinase plasminogen activator and urokinase plasminogen activator receptor inhibits prostate cancer cell invasion, survival, and tumorigenicity *in vivo*. *J Biol Chem* **280**, 36529–36540.

[34] Yoneda T (1998). Cellular and molecular mechanisms of breast and prostate cancer metastasis to bone. *Eur J Cancer* **34**, 240–245.

[35] Andreasen PA, Kjoller L, Christensen L, and Duffy MJ (1997). The urokinase-type plasminogen activator system in cancer metastasis: a review. *Int J Cancer* **72**, 1–22.

[36] Sidenius N and Blasi F (2003). The urokinase plasminogen activator system in cancer: recent advances and implication for prognosis and therapy. *Cancer Metastasis Rev* **22**, 205–222.

[37] Choong PF and Nadesapillai AP (2003). Urokinase plasminogen activator system: a multifunctional role in tumor progression and metastasis. *Clin Orthop Relat Res* (415 Suppl), S46–S58.

[38] Achbarou A, Kaiser S, Tremblay G, Ste-Marie LG, Brodt P, Goltzman D, and Rabbani SA (1994). Urokinase overproduction results in increased skeletal metastasis by prostate cancer cells *in vivo*. *Cancer Res* **54**, 2372–2377.

[39] Arens N, Gandhari M, Bleyl U, and Hildenbrand R (2005). *In vitro* suppression of urokinase plasminogen activator in breast cancer cells—a comparison of two antisense strategies. *Int J Oncol* **26**, 113–119.

[40] Salvi A, Arici B, De Petro G, and Barlati S (2004). Small interfering RNA urokinase silencing inhibits invasion and migration of human hepatocellular carcinoma cells. *Mol Cancer Ther* **3**, 671–678.

[41] Fischer K, Lutz V, Wilhelm O, Schmitt M, Graeff H, Heiss P, Nishiguchi T, Harbeck N, Kessler H, Luther T, et al. (1998). Urokinase induces proliferation of human ovarian cancer cells: characterization of structural elements required for growth factor function. *FEBS Lett* **438**, 101–105.

[42] Fishman DA, Kearns A, Larsh S, Enghild JJ, and Stack MS (1999). Autocrine regulation of growth stimulation in human epithelial ovarian carcinoma by serine-proteinase–catalysed release of the urinary-type–plasminogen-activator N-terminal fragment. *J Biochem* **341** (Pt 3), 765–769.

[43] Mahanivong C, Yu J, and Huang S (2007). Elevated urokinase-specific surface receptor expression is maintained through its interaction with urokinase plasminogen activator. *Mol Carcinog* **46**, 165–175.

[44] Knoop A, Andreasen PA, Andersen JA, Hansen S, Laenkholm AV, Simonsen AC, Andersen J, Overgaard J, and Rose C (1998). Prognostic significance of urokinase-type plasminogen activator and plasminogen activator inhibitor-1 in primary breast cancer. *Br J Cancer* **77**, 932–940.

[45] Pavey SJ, Marsh NA, Ray MJ, Butler D, Dare AJ, and Hawson GA (1996). Changes in plasminogen activator inhibitor-1 levels in non–small cell lung cancer. *Boll Soc Ital Biol Sper* **72**, 331–340.

[46] Abe J, Urano T, Konno H, Erhan Y, Tanaka T, Nishino N, Takada A, and Nakamura S (1999). Larger and more invasive colorectal carcinoma contains larger amounts of plasminogen activator inhibitor type 1 and its relative ratio over urokinase receptor correlates well with tumor size. *Cancer* **86**, 2602–2611.

[47] Gershtein ES and Kushlinskii NE (2001). Urokinase and tissue plasminogen activators and their inhibitor PAI-1 in human tumors. *Bull Exp Biol Med* **131**, 67–72.

[48] Ohba K, Miyata Y, Kanda S, Koga S, Hayashi T, and Kanetake H (2005). Expression of urokinase-type plasminogen activator, urokinase-type plasminogen activator receptor and plasminogen activator inhibitors in patients with renal cell carcinoma: correlation with tumor associated macrophage and prognosis. *J Urol* **174**, 461–465.

[49] Hundsdorfer B, Zeilhofer HF, Bock KP, Dettmar P, Schmitt M, Kolk A, Pautke C, and Horch HH (2005). Tumour-associated urokinase-type plasminogen activator (uPA) and its inhibitor PAI-1 in normal and neoplastic tissues of patients with squamous cell cancer of the oral cavity—clinical relevance and prognostic value. *J Craniomaxillofac Surg* **33**, 191–196.

[50] Usher PA, Thomsen OF, Iversen P, Johnsen M, Brunner N, Hoyer-Hansen G, Andreasen P, Dano K, and Nielsen BS (2005). Expression of urokinase plasminogen activator, its receptor and type-1 inhibitor in malignant and benign prostate tissue. *Int J Cancer* **113**, 870–880.

[51] Takahashi T, Suzuki K, Ihara H, Mogami H, Kazui T, and Urano T (2005). Plasminogen activator inhibitor type 1 promotes fibrosarcoma cell migration by modifying cellular attachment to vitronectin via alpha(v)beta(5) integrin. *Semin Thromb Hemost* **31**, 356–363.